Proceedings in Applied Mathematics and Mechanics

PAMM Proceedings in Applied Mathematics and Mechanics

SPECIAL ISSUE 95th Annual Meeting of the International Association of Applied Mathematics and Mechanics (GAMM)

RESEARCH ARTICLE OPEN ACCESS

Numerical Modeling of Inertial Particles in Three-Dimensional Fluid Flow

Vamika Rathi | Daniel Ruprecht

Chair Computational Mathematics, Institute of Mathematics, Hamburg University of Technology, Hamburg, Germany

Correspondence: Vamika Rathi (vamika.rathi@tuhh.de)

Received: 23 February 2026 | **Revised:** 15 May 2026 | **Accepted:** 19 May 2026

ABSTRACT

The motion of inertial particles in a fluid is modeled by the Maxey–Riley–Gatignol equation (MaRGE). The MaRGE contains an integral term that arises due to the viscous diffusion of vorticity in the fluid around the particle. Because it makes MaRGE difficult to solve numerically, the integral term is often neglected or approximated, despite its demonstrated importance for obtaining realistic trajectories. There are some studies that propose algorithms to solve the full MaRGE numerically for two dimensional flows fields. For simple flows like a vortex, analytical solutions exist that can serve as test cases to verify implementations. However, in most practical applications, fluids will be three dimensional. This article extends a multi-step algorithm proposed by Daitche to the three-dimensional case. Based on an approach by Candelier et al., it derives an analytical solution for a particle moving in a three-dimensional vortex while being subject to gravity. Numerical examples compare empirical and theoretical convergence orders and demonstrate order reduction in particular for particles with non-zero relative initial velocity.

1 | Introduction

Modeling inertial particles moving in a fluid is an important problem, arising in the study of, for example, spread of wildfires [1], dispersion of COVID-19 virus through spherical droplets [2], multiphase flows [3], dynamics of prey for feeding marine animals like jellyfish [4], and more. The equation of motion for a spherical inertial particle of radius a and mass m_p is

$$\begin{aligned} m_p\dot{\boldsymbol{v}} = \; & m_f\frac{\mathrm{D}\boldsymbol{u}}{\mathrm{D}t} - \frac{m_f}{2}\left[\dot{\boldsymbol{v}} - \frac{\mathrm{D}\boldsymbol{u}}{\mathrm{D}t}\right] - 6\pi a\rho_f\nu(\boldsymbol{v}-\boldsymbol{u}) \\ & - 6a^2\rho_f\sqrt{\pi\nu}\left[\int_{t_0}^{t}\frac{\dot{\boldsymbol{v}}(\tau)-\dot{\boldsymbol{u}}(\tau)}{\sqrt{t-\tau}}\mathrm{d}\tau + \frac{\boldsymbol{v}(t_0)-\boldsymbol{u}(t_0)}{\sqrt{t-t_0}}\right] \\ & - (m_p - m_f)\boldsymbol{g}, \end{aligned} \tag{1}$$

and was proposed by Maxey, Riley, and Gatignol [5, 6]. Here, $\dot{\boldsymbol{x}} = \boldsymbol{v}(t)$ is the particle's absolute velocity, m_f is the mass of the fluid displaced by the particle, $\boldsymbol{u}(\boldsymbol{x}(t), t)$ is the fluid velocity at the particle's position $\boldsymbol{x}(t)$, D/D t is the material derivative, ρ_f is the fluid density, ν is the kinematic viscosity of the fluid, and $\boldsymbol{g}$ is the gravitational force vector. We ignore the Faxén correction terms since they are smaller in magnitude than the other forces [7] but they become relevant for very large particles.

The terms on the right-hand side of (1) model the force exerted by the undisturbed fluid, the added mass term, the Stokes drag, the history force due to memory effects of the particle moving in a viscous fluid and the buoyancy force. The integral term, also called Basset history term, turns the MaRGE into an integro-differential equation and makes it challenging to solve numerically. Therefore, it is often neglected despite both experimental [8] and analytical [9] evidence that its effects are not negligible, not only for single particles but also for large scale Lagrangian dynamics and clustering patterns [10].

The local existence and uniqueness of weak solutions to (1) was proved by Farazmand and Haller [11] and later extended to global existence [12, 13]. They also show that for zero relative initial

velocity, these weak solutions are classically differentiable and hence become strong solutions. Crisan and Street show that these two statements are equivalent and that solutions always lack classical differentiability for non-zero initial relative velocity [13]. Together with a stiff relaxation towards the flow field velocity for large Stokes numbers, this leads to order reduction of numerical methods based on the differential form of MaRGE [14].

Numerical algorithms have been developed that solve the full MaRGE without approximations. In 2013, Daitche developed numerical schemes up to order three for 2D MaRGE based on multi-step methods [15]. Moreno-Casas and Bombardelli [16] review methods based on quadrature schemes and variants of window based approaches. Prasath et al. [9] proposed an alternative approach, demonstrating that the full MaRGE can be reformulated as a dynamic boundary condition of a one-dimensional diffusion equation on a one-dimensional, semi-infinite domain. They introduce a numerical algorithm based on collocation for the transformed problem. Their algorithm delivers very high precision but is computationally expensive and, in some situations, finite difference based approaches can be more efficient [14]. Jaganathan et al. [17] transform the inherent non-Markovian system of MaRGE into a Markovian form, which facilitates efficient numerical integration. While all these methods can be extended to 3D flow fields, we use Daitche's method here because it is straightforward to implement.

For verification of numerical schemes, testcases with analytical solutions are indispensable. Candelier et al. [8] provide a solution to (1) when $\boldsymbol{u}$ is a simple 2D vortex flow field. Prasath et al. [9] derive solutions for a relaxing particle when $\boldsymbol{u} = 0$ with and without gravity and for a particle in a spatially homogeneous, time-periodic flow. However, no analytical testcases for 3D flow fields seem to exist in the literature. In this article, we extend the method by Daitche to 3D MaRGE and present an analytical solution for a particle that is less dense than the fluid and subject to gravity in a three-dimensional vortex flow.

2 | Numerical Solution of MaRGE in Three-Dimensional Flow Fields

Equation (1) is in dimensional form where all quantities have physical units. In order to find a numerical solution, we nondimensionalize it by introducing a characteristic time T, a characteristic velocity U and a characteristic length $L = UT$. We introduce the dimensionless length, time, and velocity

$$\bar{x} = x/L, \qquad \bar{t} = t/T, \qquad \bar{\boldsymbol{v}} = \boldsymbol{v}/U, \qquad \bar{\boldsymbol{u}} = u/U.$$

The dimensionless form of (1)

$$\frac{\mathrm{d}\bar{\boldsymbol{v}}}{\mathrm{d}\bar{t}} = R\,\frac{\mathrm{D}\bar{\boldsymbol{u}}}{\mathrm{D}\bar{t}} - \frac{R}{S}(\bar{\boldsymbol{v}} - \bar{\boldsymbol{u}}) - R\sqrt{\frac{3}{S\pi}}\frac{\mathrm{d}}{\mathrm{d}\bar{t}}\int_{\bar{t}_0}^{\bar{t}} \frac{1}{\sqrt{\bar{t}-\tau}}(\bar{\boldsymbol{v}} - \bar{\boldsymbol{u}})\mathrm{d}\tau - (1-R)\boldsymbol{G}, \tag{2}$$

is given, for example, by Daitche [15]. Here, R is the density ratio parameter, S is the ratio of particle's viscous relaxation time to T, which we call Stokes number, and $\boldsymbol{G}$ is the dimensionless gravitational vector

$$R = \frac{3m_f}{m_f + 2m_p}, \qquad S = \frac{1}{3}\frac{a^2/\nu}{T}, \qquad \boldsymbol{G} = \frac{T}{U}\boldsymbol{g}. \tag{3}$$

The history term in (2) is modified using the identity

$$\int_{t_0}^{t} \frac{1}{\sqrt{t-\tau}}\frac{\mathrm{d}}{\mathrm{d}\tau}f(\tau)\mathrm{d}\tau + \frac{f(\tau_0)}{\sqrt{t-\tau}} = \frac{\mathrm{d}}{\mathrm{d}t}\int_{t_0}^{t}\frac{f(\tau)}{\sqrt{t-\tau}}\mathrm{d}\tau,$$

where $f(\tau) = \boldsymbol{v} - \boldsymbol{u}$, which follows by first differentiating and then using integration by parts [18].

Since we only consider dimensionless quantities from now on, we drop the overbar from (2). Daitche [15] introduced first-, second-, and third-order schemes based on quadrature schemes and linear multi-step methods for 2D MaRGE. Here, we extend his method to the three-dimensional case and also discuss how to treat the gravitational force vector. First, we rewrite (2) for the relative velocity $\boldsymbol{w} = \boldsymbol{v} - \boldsymbol{u}$ of the particle

$$\frac{\mathrm{d}\boldsymbol{w}}{\mathrm{d}t} = (R-1)\,\frac{\mathrm{d}\boldsymbol{u}}{\mathrm{d}t} - R\,\boldsymbol{w}\cdot\nabla\boldsymbol{u} - \frac{R}{S}\,\boldsymbol{w} - R\sqrt{\frac{3}{S\pi}}\frac{\mathrm{d}}{\mathrm{d}t}\int_{t_0}^{t}\frac{\boldsymbol{w}(\tau)}{\sqrt{t-\tau}}\mathrm{d}\tau - (1-R)\boldsymbol{G}. \tag{4}$$

The equation for particle position is

$$\frac{\mathrm{d}\boldsymbol{x}}{\mathrm{d}t} = \boldsymbol{v} = \boldsymbol{w} + \boldsymbol{u}. \tag{5}$$

Let

$$\mathbb{G} = (R-1)\,\frac{\mathrm{d}\boldsymbol{u}}{\mathrm{d}t} - R\,\boldsymbol{w}\cdot\nabla\boldsymbol{u} - \frac{R}{S}\,\boldsymbol{w} - (1-R)\boldsymbol{G},$$

$$\mathbb{H} = -R\sqrt{\frac{3}{S\pi}}\int_{t_0}^{t}\frac{\boldsymbol{w}(\tau)}{\sqrt{t-\tau}}\mathrm{d}\tau.$$

Integrating (4) from t to $t+h$, where h is the step size, we get

$$\boldsymbol{w}(t+h) = \boldsymbol{w}(t) + \int_{t}^{t+h}\mathbb{G}(\tau)\mathrm{d}\tau + \mathbb{H}(t+h) - \mathbb{H}(t). \tag{6}$$

The integral term in $\mathbb{H}$ is approximated using specially developed quadrature schemes, which can be written as

$$\int_{t_0}^{t}\frac{\boldsymbol{w}(\tau)}{\sqrt{t-\tau}}\mathrm{d}\tau = \sqrt{h}\sum_{j=0}^{N}\eta_j^N\boldsymbol{w}(\tau_{N-j}) + \mathcal{O}(h^m)\sqrt{t-t_0}, \tag{7}$$

where N is the number of intervals for approximation and the coefficients η_j^N are calculated using polynomial approximations according to required order m. In Equation (7), $\tau_k = t_0 + hk$ and $h = (t-t_0)/N$. The expressions for first-, second-, and third-order coefficients are lengthy and can be found in [15]. Combining this with one-, two- and three-step Adams–Bashforth methods to approximate the integral over $\mathbb{G}$, and matching these with the corresponding order quadrature schemes for $\mathbb{H}$, we obtain first-, second-, and third-order numerical schemes for the full 3D MaRGE.

3 | Analytical Solution for a Particle in a Three-Dimensional Vortex With Gravity

To provide the means to verify any implementation of a three-dimensional MaRGE numerical solver, we derive an analytical solution for a particle moving in a vortex flow field

$$\boldsymbol{u} = \omega \begin{bmatrix} -y \\ x \\ 0 \end{bmatrix}, \tag{8}$$

with angular velocity ω while being subject to gravity. The analytical solution of MaRGE in a 2D vortex flow with assumed initial no-slip condition is given by Candelier et al. [8]. We write the non-dimensional MaRGE (2) with flow field (8) component-wise as

$$\ddot{x}(t) = -\frac{3}{2\gamma+1}x(t) - \frac{1}{(2\gamma+1)S_p}(\dot{x}(t)+y(t)) + \frac{3}{(2\gamma+1)\sqrt{\pi S_p}}\int_0^t \frac{-\dot{y}(\tau)-\ddot{x}(\tau)}{\sqrt{t-\tau}}\mathrm{d}\tau, \tag{9a}$$

$$\ddot{y}(t) = -\frac{3}{2\gamma+1}y(t) - \frac{1}{(2\gamma+1)S_p}(\dot{y}(t)-x(t)) + \frac{3}{(2\gamma+1)\sqrt{\pi S_p}}\int_0^t \frac{\dot{x}(\tau)-\ddot{y}(\tau)}{\sqrt{t-\tau}}\mathrm{d}\tau, \tag{9b}$$

$$\ddot{z}(t) = \frac{1-\gamma}{2\gamma+1}\frac{2}{Fr} - \frac{1}{(2\gamma+1)S_p}\dot{z}(t) + \frac{3}{(2\gamma+1)\sqrt{\pi S_p}}\int_0^t \frac{-\ddot{z}(\tau)}{\sqrt{t-\tau}}\mathrm{d}\tau, \tag{9c}$$

where $\dot{X} = \mathrm{d}X/\mathrm{d}t$, $\gamma = \rho_p/\rho_f$ and $\rho_p = 1/m_p$ and $\rho_f = 1/m_f$ are the particle and fluid density. Furthermore,

$$S_p = \frac{a^2\omega}{9\nu}, \qquad \mathrm{Fr} = \frac{R^2\omega}{g}, \tag{10}$$

where S_p is the pseudo-Stokes number and Fr is the pseudo-Froude number. In (9), the motion along z is decoupled from the motion in the (x, y) plane. Candelier et al. solved the MaRGE in the (x, y) plane using Laplace transforms. By writing $Z(t) = x(t) + iy(t)$ and $U(t) = \dot{Z}(t)$, they write (9a) and (9b) as

$$\dot{U} + AU + B\left[\int_0^t U(\tau)\mathrm{d}\tau + Z(0)\right] + C\int_0^t \frac{-\dot{U}(\tau)+iU(\tau)}{\sqrt{t-\tau}}\mathrm{d}\tau = 0, \tag{11}$$

where

$$A = \frac{1}{(2\gamma+1)S_p}, \qquad B = \frac{3S_p - i}{(2\gamma+1)S_p}, \qquad C = -\frac{3}{(2\gamma+1)\sqrt{\pi S_p}}. \tag{12}$$

Using Laplace transform, partial fraction decomposition and then calculating inverse Laplace transform, they get the solution

$$Z(t) = \sum_{i=1}^{4}\frac{A_i}{X_i}\exp(X_i^2 t)\mathrm{erfc}(-X_i\sqrt{t}), \tag{13}$$

where A_i and X_i are given in the appendices of [8]. We follow a similar process to solve the equation for z-component. Taking $U_z(t) = \dot{z}(t)$, Equation (9c) becomes

$$\dot{U}_z + AU_z - D - C\int_0^t \frac{-\dot{U}_z(\tau)}{\sqrt{t-\tau}}\mathrm{d}\tau = 0, \tag{14}$$

where A and C are as given in (12) and D is

$$D = \frac{1-\gamma}{2\gamma+1}\frac{2}{Fr}. \tag{15}$$

The Laplace transform of (14) is

$$\tilde{U}_z(s)\left(s + A - C\sqrt{\pi}\sqrt{s}\right) = \frac{D}{s} - C\sqrt{\frac{\pi}{s}}U_z(0) + U_z(0), \tag{16}$$

where $\tilde{U}_z(s)$ denotes the Laplace transform of $U_z(t)$. Let $V = \sqrt{s}$, so that

$$\tilde{U}_z(s) = \frac{U_z(0)(V^2 - C\sqrt{\pi}V) + D}{V^4 - C\sqrt{\pi}V^3 + AV^2}. \tag{17}$$

Since the flow field (8) has no velocity in vertical direction and we have to assume zero relative initial velocity, the particle starts with the velocity same as the fluid velocity so that that $U_z(0) = \dot{z}(0) = 0$. To calculate the inverse Laplace transform of $\tilde{U}_z(s)$, we need the partial fraction decomposition

$$\tilde{U}_z(s) = \frac{DC\sqrt{\pi}}{A^2\sqrt{s}} + \frac{D}{As} + \frac{E_1}{\sqrt{s}-V_1} + \frac{E_2}{\sqrt{s}-V_2}, \tag{18}$$

where

$$V_1 = \frac{\sqrt{\pi}C + \sqrt{C^2\pi - 4A}}{2}, \quad V_2 = \frac{\sqrt{\pi}C - \sqrt{C^2\pi - 4A}}{2}, \tag{19}$$

and

$$E_1 = \frac{D(-C^2\pi + 2A - C\sqrt{\pi}\sqrt{C^2\pi - 4A})}{2A^2\sqrt{C^2\pi - 4A}}, \qquad E_2 = \frac{D(C^2\pi - 2A - C\sqrt{\pi}\sqrt{C^2\pi - 4A})}{2A^2\sqrt{C^2\pi - 4A}}. \tag{20}$$

Note that we need the condition $C^2\pi - 4A > 0$, that is, $\gamma < 5/8$, that is, $\rho_p/\rho_f < 5/8$ to be satisfied. The inverse Laplace transform of $\tilde{U}_z(s)$ is

$$U_z(t) = \frac{DC}{A^2\sqrt{t}} + \frac{D}{A} + \sum_{i=1}^{i=2} E_i V_i \exp({V_i}^2 t)\mathrm{erfc}(-V_i\sqrt{t}), \tag{21}$$

where $\exp({V_i}^2 t)\mathrm{erfc}(-V_i\sqrt{t})$ is a special case of Mittag–Leffler functions $E_\alpha(V_i\sqrt{t})$ with $\alpha = 1/2$ and, by integrating $U_z(t)$, we obtain

$$z(t) = 2\frac{DC}{A^2}\sqrt{t} + \frac{D}{A}t + \sum_{i=1}^{i=2} E_i \times \left(\frac{1}{V_i}\exp({V_i}^2 t)\mathrm{erfc}(-V_i\sqrt{t}) - \frac{1}{V_i}\right) + z(0). \tag{22}$$

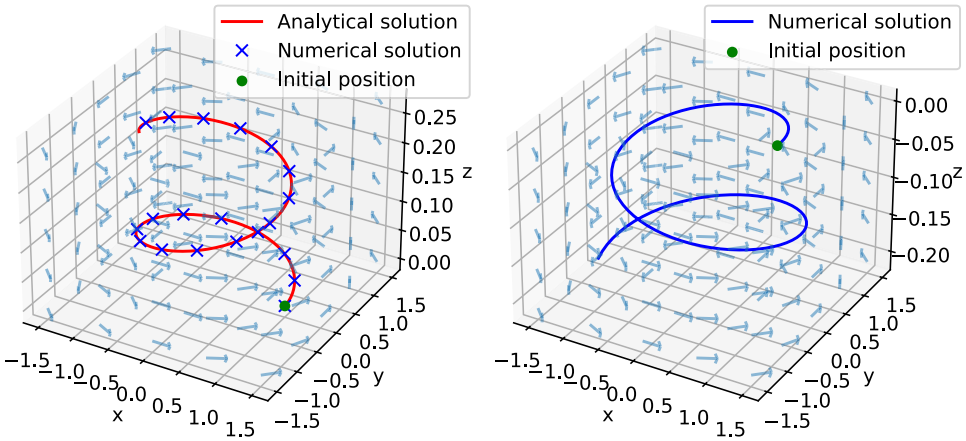

FIGURE 1 | Flow field $\boldsymbol{u}$(arrows), numerical solution of MaRGE computed with Daitche's method (blue) and analytical solution (red). The left figure is for a particle with density that is smaller than the fluid density, the right for a particle with density greater than the fluid.

The function erfc, also called complementary error function, is defined as $\mathrm{erfc}(t) = 1 - \mathrm{erf}(t)$, where $\mathrm{erf}(t) = \frac{2}{\sqrt{\pi}} \int_0^t e^{-\tau^2} \mathrm{d}\tau$ is the error function. Equation (13) along with (22) gives the analytical solution for 3D MaRGE, but only for particles that satisfy $\rho_p/\rho_f < 5/8$.

Note that for velocity fields with a non-zero vertical component and $\dot{z}(0) = U_z(0) \neq 0$, the numerator of (17) can be written as

$$U_z(0)(V^2 - C\sqrt{\pi}V) + D = \underbrace{(D - AU_z(0))}_{\equiv D^*} + U_z(0)\underbrace{(V^2 - C\sqrt{\pi}V + A)}_{\text{denominator factor}}, \quad (23)$$

which gives the partial fraction decomposition

$$\tilde{U}_z(s) = \frac{D^* C\sqrt{\pi}}{A^2\sqrt{s}} + \frac{D}{As} + \frac{\tilde{E}_1}{\sqrt{s} - V_1} + \frac{\tilde{E}_2}{\sqrt{s} - V_2}, \quad (24)$$

where $\tilde{E}_i = (D^*/D)\, E_i$. This can be solved similarly, giving

$$U_z(t) = \frac{D^* C}{A^2\sqrt{t}} + \frac{D}{A} + \sum_{i=1}^{2} \tilde{E}_i V_i \exp(V_i^2 t)\, \mathrm{erfc}(-V_i\sqrt{t}). \quad (25)$$

4 | Numerical Examples

Figure 1 shows the flow field (8) as arrows. The figure on the left shows the analytical solution (in red) with a numerical solution represented by blue crosses for a particle that is less dense than the fluid and thus rises upwards. The figure on the right shows the trajectory of particle denser than the fluid, which travels downwards under the influence of gravity. In both cases, the initial relative velocity of the particle is zero and the green dot represents its initial position. The particle radius is 1.5 mm and times are $t \in [0, 10]$. The fluid density is 972 kg m^{-3}, the particle density for the heavier particle is 1410 kg m^{-3} and for the lighter particle, 500 kg m^{-3}. The kinematic viscosity of the fluid is 2×10^{-4} m^2 s^{-1}, as in Candelier et al. [8]. For the analytical and numerical solutions to agree, we need to consider the same characteristic values for both which, again following Candelier [8], we set to $T = 0.1$, $L = 0.04$ and $U = L/T = 0.4$.

4.1 | Positively Buoyant Particle

Figures 2 and 3 show L_∞ error versus the total number of time steps N for the particle that is less dense than the fluid with zero (Figure 2) and non-zero initial (Figure 3) relative velocity and Stokes numbers $S = 3$ (left) and $S = 0.3$ (right). For zero relative initial velocity, the error is computed against the analytical solution while for non-zero relative initial velocity the error is estimated by computing the difference to a higher resolution numerical solution.

If $\boldsymbol{w}(0) = 0$, we get first and second order convergence from the corresponding variants of Daitche's method as expected. The third-order variant converges with order somewhere between two and three but is significantly more accurate than the second-order variant. If the initial velocity of the particle does not match the velocity of the flow field at its initial position and thus $\boldsymbol{w}(0) \neq 0$, convergence becomes significantly worse. The first order variant matches is theoretical order of convergence but second- and third-order variant converge with an order of only slightly more than one. Note also that in both cases the errors are slightly higher for $S = 0.3$ compared to $S = 3$, likely because the timescale of relaxation toward the flow field velocity is shorter for a particle with a smaller Stokes number, making the problem stiffer.

4.2 | Negatively Buoyant Particle

Figures 4 and 5 show the L_∞-error against the number of time-steps for zero (upper) and non-zero (lower) initial relative velocity and Stokes numbers $S = 3$ (left) and $S = 0.3$ (right). Since the analytical solution is only valid for particles that are less dense than the fluid, we always compute the error by comparing against a higher resolution numerical reference here.

Again, if $\boldsymbol{w}(0) = 0$, the first- and second-order variant of Daitche's method achieve their theoretically expected convergence order.

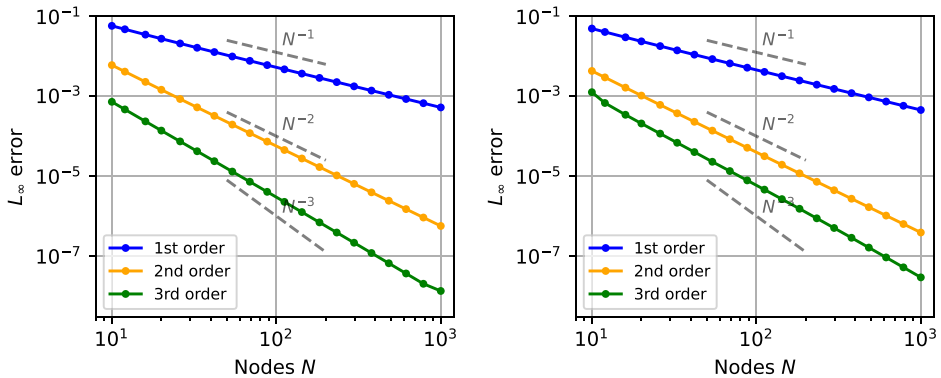

FIGURE 2 | Error against the analytical solution versus number of time steps for a particle that is lighter than the fluid for the first-, second-, and third-order variant of Daitche's method. The initial relative velocity is zero, the initial position is (1,0,0) and $t \in [0, 1]$. The Stokes number of the particle is $S = 3$ (left) and $S = 0.3$ (right).

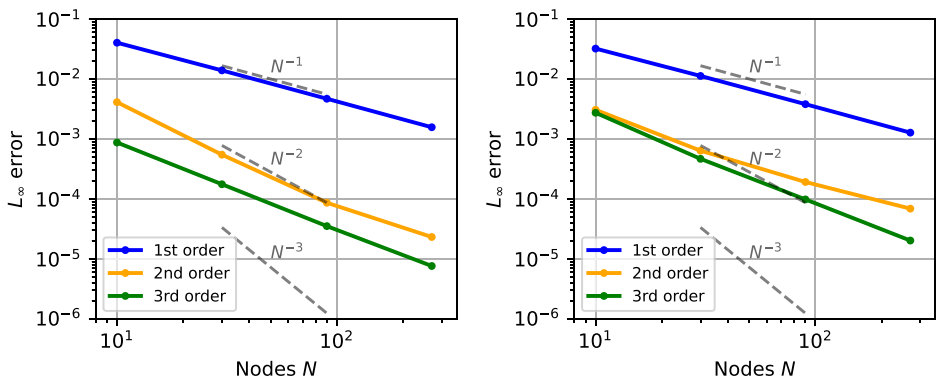

FIGURE 3 | Error against a numerically computed reference solution versus number of time steps for a particle that is lighter than the fluid for the first-, second-, and third-order variant of Daitche's method. The initial relative velocity is (0,0.1,0), the initial position is (1,0,0) and $t \in [0, 1]$. The Stokes number of the particle is $S = 3$ (left) and $S = 0.3$ (right). Order reduction from increasing stiffness as the Stokes number gets smaller is visible for the third-order method in the right plot.

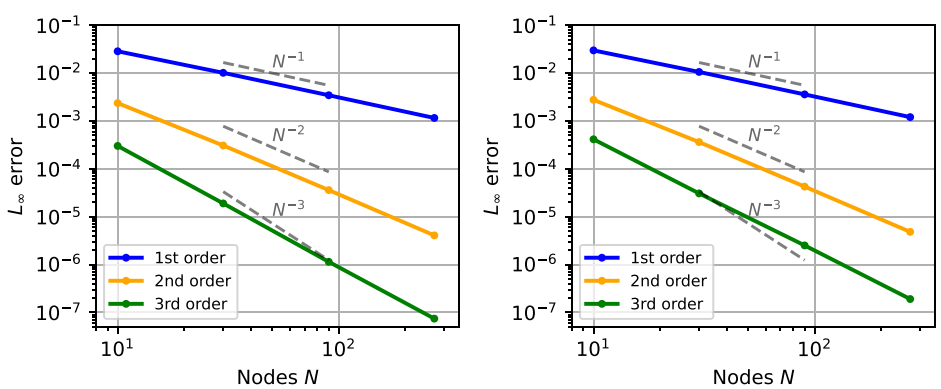

FIGURE 4 | Error against a numerically computed reference solution versus number of time steps for a particle that is heavier than the fluid for the first-, second-, and third-order variant of Daitche's method. The initial relative velocity is zero, the initial position is (1,0,0) and $t \in [0, 1]$. The Stokes number of the particle is $S = 3$ (left) and $S = 0.3$ (right).

The third-order variant is not quite of order three but more accurate than the second-order version. A non-zero relative initial velocity again causes order reduction for the second- and third-order variant. As before, errors are slightly higher for the particle with Stokes number $S = 0.3$.

5 | Conclusion

The MaRGE models the motion of spherical inertial particles immersed in a fluid. While numerical solvers and analytical solutions exist for two-dimensional flow fields, for most practical

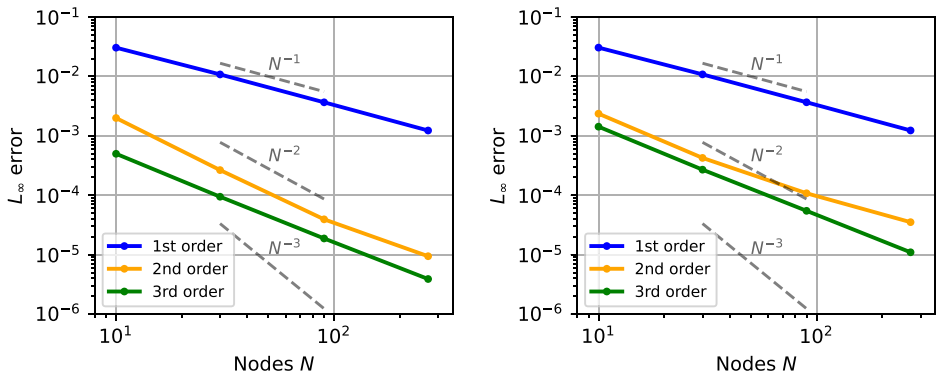

FIGURE 5 | Error against a numerically computed reference solution versus number of time steps for a particle that is heavier than the fluid for the first-, second-, and third-order variant of Daitche's method. The initial relative velocity is (0,0.1,0), the initial position is (1,0,0) and $t \in [0, 1]$. The Stokes number of the particle is $S = 3$ (left) and $S = 0.3$ (right). Order reduction from the rapid stiff adjustment due to the non-zero initial relative velocity is visible in both cases.

applications, their solution is needed for 3D flows. We present a numerical solver for the 3D MaRGe using the quadrature schemes for solving the history term and Adams–Bashforth methods proposed by Daitche [15]. An analytical solution for MaRGE for a two-dimensional vortex was derived by Candelier [8], which we extend to a particles with a small density ratio moving in 3D in a vortex while being subject to gravity. We investigate the convergence order of our numerical scheme for particles with different density, Stokes number and with zero and non-zero initial relative velocity. Generalizing the analytical solution to particles of any density would be an interesting direction for future research.

Acknowledgments

This project is funded by the Deutsche Forschungsgemeinschaft (DFG, German Research Foundation) – SFB 1615 – 503850735.

Open access funding enabled and organized by Projekt DEAL.

References

1. A. Mendez and M. Farazmand, "Quantifying Rare Events in Spotting: How Far Do Wildfires Spread?" *Fire Safety Journal* 132 (2022): 103630.

2. C. P. Cummins, O. J. Ajayi, F. V. Mehendale, R. Gabl, and I. M. Viola, "The Dispersion of Spherical Droplets in Source–Sink Flows and Their Relevance to the COVID-19 Pandemic," *Physics of Fluids* 32, no. 8 (2020): 083302.

3. S. Balachandar and J. K. Eaton, "Turbulent Dispersed Multiphase Flow," *Annual Review of Fluid Mechanics* 42, no. 1 (2010): 111–133.

4. T. Sapsis, J. Peng, and G. Haller, "Instabilities on Prey Dynamics in Jellyfish Feeding," *Bulletin of Mathematical Biology* 73, no. 8 (2011): 1841–1856.

5. M. R. Maxey and J. J. Riley, "Equation of Motion for a Small Rigid Sphere in a Nonuniform Flow," *Physics of Fluids* 26, no. 4 (1983): 883–889.

6. R. Gatignol, "The Faxén Formulae for a Rigid Particle in an Unsteady Non-Uniform Stokes Flow," *Journal de Mécanique Théorique et Appliquée* 2, no. 2 (1983): 143–160.

7. R. Mei, R. J. Adrian, and T. J. Hanratty, "Particle Dispersion in Isotropic Turbulence under Stokes Drag and Basset Force With Gravitational Settling," *Journal of Fluid Mechanics* 225 (1991): 481–495.

8. F. Candelier, J. R. Angilella, and M. Souhar, "On the Effect of the Boussinesq–Basset Force on the Radial Migration of a Stokes Particle in a Vortex," *Physics of Fluids* 16, no. 5 (2004): 1765–1776.

9. S. G. Prasath, V. Vasan, and R. Govindarajan, "Accurate Solution Method for the Maxey–Riley Equation, and the Effects of Basset History," *Journal of Fluid Mechanics* 868 (2019): 428–460.

10. J. Urizarna-Carasa, D. Ruprecht, A. von Kameke, and K. Padberg-Gehle, "Relevance of the Basset History Term for Lagrangian Particle Dynamics," *Chaos: An Interdisciplinary Journal of Nonlinear Science* 35, no. 7 (2025): 073122.

11. M. Farazmand and G. Haller, "The Maxey–Riley Equation: Existence, Uniqueness and Regularity of Solutions," *Nonlinear Analysis: Real World Applications* 22 (2015): 98–106.

12. G. P. Langlois, M. Farazmand, and G. Haller, "Asymptotic Dynamics of Inertial Particles With Memory," *Journal of Nonlinear Science* 25 (2015): 1225–1255.

13. D. Crisan and O. D. Street, "On the Analytical Aspects of Inertial Particle Motion," *Journal of Mathematical Analysis and Applications* 516, no. 1 (2022): 126467.

14. J. Urizarna-Carasa, L. Schlegel, and D. Ruprecht, "Efficient Numerical Methods for the Maxey–Riley–Gatignol Equations With Basset History Term," *Computer Physics Communications* 310 (2025): 109502.

15. A. Daitche, "Advection of Inertial Particles in the Presence of the History Force: Higher Order Numerical Schemes," *Journal of Computational Physics* 254 (2013): 93–106.

16. P. A. Moreno-Casas and F. A. Bombardelli, "Computation of the Basset Force: Recent Advances and Environmental Flow Applications," *Environmental Fluid Mechanics* 16, no. 1 (2016): 193–208.

17. D. Jaganathan, R. Govindarajan, and V. Vasan, "Explicit Runge–Kutta Algorithm to Solve Non-Local Equations With Memory Effects: Case of the Maxey–Riley–Gatignol Equation," *Quarterly of Applied Mathematics* 83, no. 1 (2024): 135–158.

18. I. Podlubny, *Fractional Differential Equations: An Introduction to Fractional Derivatives, Fractional Differential Equations, to Methods of Their Solution and Some of Their Applications* (Academic Press, 1998).